Observed Structure of Spray Detonations

K. W. RAGLAND,* E. K. DABORA,† AND J. A. NICHOLLS
Gas Dynamics Laboratories, Department of Aerospace Engineering
The University of Michigan, Ann Arbor, Michigan
(Received 18 December 1967; final manuscript received 10 July 1968)

The propagation of a detonation wave in a tube containing a single stream of 2600-μ-diam diethylcyclohexane droplets dispersed in gaseous oxygen has been studied with streak and space resolved photography, special pressure transducers, and thin-film heat-transfer gauges. The detonation wave, which reached a velocity of 4100 ft/sec, consisted of a planar shock front followed by secondary shocks and a gradual decrease in pressure as heat is added. A detailed history of an individual drop within the reaction zone is presented. Under the observed conditions a 2600-μ-drop disintegrates continuously over a period of 500 μsec. Combustion is initiated in the wake of the drops at 65 μsec after the passage of the shock with the reaction zone considered completed in 670 μsec. One-dimensional equations for a two-phase Chapman–Jouguet detonation wave with mass and heat addition within the reaction zone, and momentum and heat transfer out of the reaction zone are derived. Comparison of the experiments with the theoretical prediction yields a reasonable agreement.

I. INTRODUCTION

In contrast to gaseous detonation waves, which were discovered about 85 years ago, it has only recently been recognized that a detonation wave can exist in a medium consisting of liquid fuel droplets dispersed in a gaseous oxidizer. Since an over-all stoichiometric mixture may be obtained with a dilute spray (i.e., the ratio of the volume occupied by the liquid to the volume occupied by the gas is less than 10^{-3} for most mixtures of interest), there is no conceptual difficulty associated with the propagation of the shock front of the detonation wave through the medium. However, because the reaction zone of a gaseous detonation is completed in the order of 5 μsec or less, one is tempted to assume that fuel from the droplets cannot enter into an exothermic chemical reaction rapidly enough to allow a steady-state detonation wave to propagate through a two-phase, liquid–gas media. Indeed, data on the dynamic behavior of a liquid droplet in a supersonic, high-pressure, convective flow that would be associated with the reaction zone of a detonation wave have not been available.

Williams[1] analyzed the structure of a "laminar" detonation wave in a dilute spray by assuming a heterogeneous reaction mechanism such that the nonvolatile fuel burned to completion in the surface layer of the droplet. An ideal gas with constant average molecular weight, and constant and equal specific heats for each species was assumed. The Stokes' drag law and a semiempirical droplet burning rate law assuming no stripping or shattering of the drop were used. From an order of magnitude analysis Williams showed that a model analogous to that of Zeldovich, von Neumann, and Doring[2] for a gaseous detonation was reasonable. However, the length of the reaction zone for 30-μ-diam drops was of the order of 100 cm so that he felt that the interaction of the deflagration zone with the walls would be stronger than its interaction with the shock wave. Thus, without being able to assess the effect of the breakup of the drops by the convective flow behind the initial shock front, the conclusion was that the drops would probably have to be less than 10 μ in order to sustain a detonation.

Webber[3] was apparently the first to experimentally investigate the combustion of a spray when subjected to a shock wave. Kerosene or heavy mineral oil was sprayed into a vertical shock tube, and it was found that a shock was sustained and accelerated by combustion of the droplets. Cramer[4] continued the work of Webber using polydisperse sprays of diethylcyclohexane with an estimated mean diameter of 200 μ. The combustion process was termed detonationlike, but no attempt was made to apply the Rankine–Hugoniot relations and no details of the reaction zone were resolved. Further experiments on the propagation of a shock wave through a polydisperse fuel spray by Dabora, Ragland, and Nicholls[5] showed that the process could be approxi-

* Presently with the Department of Mechanical Engineering, University of Wisconsin, Madison, Wisconsin.
† Presently with the Department of Aerospace Engineering, The University of Connecticut, Storrs, Connecticut.
[1] F. A. Williams, Phys. Fluids 4, 1434 (1961).
[2] F. A. Williams, *Combustion Theory* (Addison-Wesley Publishing Company, Reading, Massachusetts, 1965), p. 147.
[3] W. T. Webber, in *Eighth International Symposium on Combustion* (The Williams and Wilkins Company, Baltimore, 1962), p. 1129.
[4] F. B. Cramer, in *Ninth International Symposium on Combustion* (Academic Press Inc., New York, 1963), p. 482.
[5] E. K. Dabora, K. W. Ragland, and J. A. Nicholls, Astronautica Acta 12, 9 (1966).

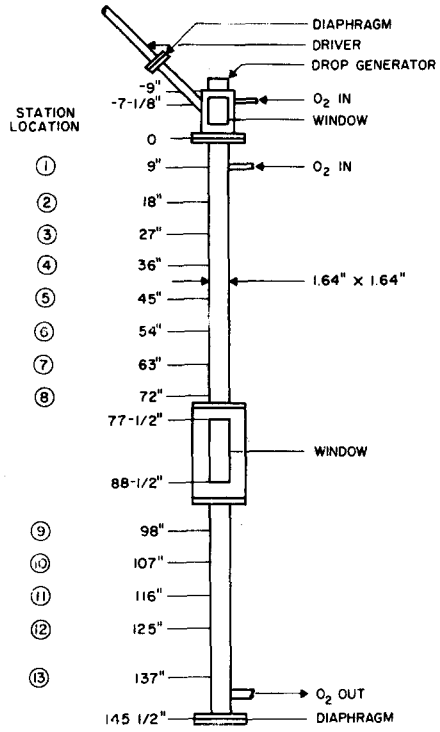

FIG. 1. Test setup for the droplet detonations.

mately described by the Rankine–Hugoniot relations (extended to two-phase flow) with the Chapman–Jouguet condition.

In order to achieve an understanding of the features of the reaction zone of a two-phase detonation it is desirable to use a monodisperse droplet field, and to insure that no fuel wets the walls of the tube.[6] Spatially resolved schlieren photographs of the combustion of a field of 940-μ-diam drops[5] showed that the reaction zone consisted of a discrete near-normal shock front followed by a region of mechanical breakup and combustion of the drops. Further experiments[7] have shown that a steady-state detonation can be established in near-stoichiometric mixtures of uniform size fuel droplets of 290 to 2600 μ dispersed in gaseous oxygen. As the size of the droplets is increased, while the mixture ratio is held constant, the details of the reaction zone may be more readily observed. This paper will present the results obtained with 2600-μ-diam drops, which is the largest size that has been studied to date, but there is no reason to believe that larger droplets could not be used.

[6] It has been shown that a tube which is coated with a thin layer of liquid and is filled only with oxygen can also support a two phase detonation. See Ref. 5 and K. W. Ragland, Ph.D. thesis, The University of Michigan (1967).

[7] E. K. Dabora, K. W. Ragland, and J. A. Nicholls, in *Twelfth Symposium (International) on Combustion* (Combustion Institute, Pittsburgh, Pennsylvania) (to be published).

It should be noted that the behavior of a particular drop within the reaction zone of a two-phase detonation is influenced by the neighboring drops. For example, a stoichiometric mixture of 250-μ-diam diethylcyclohexane drops in oxygen at standard temperature and pressure requires about 60 drops/cm^3 so that the drops are spaced about 0.25 cm apart, while 2600-μ diam drops require 17 cm^3 of oxygen per drop or approximately 2.5 cm between drops. Under these conditions, due to the convective flow within the reaction zone, with 250-μ drops the wake from the neighboring upstream drop will interact with the drop just swept over by the shock in the order of 2 μsec, while in the latter case, it will take at least 20 μsec before any interaction occurs. In both cases this represents less than 10% of the total reaction time. Thus, the neighboring drops influence the history of an individual drop because of the convective flow. In addition, it will be seen that an individual drop is affected by secondary shock waves which are generated by neighboring droplets.

The purpose of this paper is to describe the history of an individual fuel drop within the reaction zone of a two-phase detonation as obtained from photographic records, and pressure and heat-transfer measurements, and to relate this to the over-all structure of the detonation wave. Since combustion may apparently occur under certain conditions for nearly 3 ft behind the initial shock front, the Rankine–Hugoniot relations are modified in order to account for heat and momentum transfer out of the reaction zone as well as mass and heat addition within the reaction zone. Finally, the predicted propagation velocity and pressure at the end of the reaction zone are compared with the experimental measurements.

II. APPARATUS

A diagram of the combustion-tube, drop-generator, and shock-tube initiator is shown in Fig. 1. The vertical combustion tube has a square cross section of 1.64 by 1.64 in. with 0.125-in. radii on the corners and is made of 1020 welded steel, $\frac{3}{16}$in. thick. In all, the combustion tube is 13 ft long and has two flanged optical sections—one for viewing the initial formation of the drops and one for photographing the combustion. The lower optical section was machined from a solid billet of aluminum and has square corners, and was fitted with 0.75-in.-thick plate glass.

Drops of uniform size are produced at the top of the combustion tube by the drop generator and

fall freely through quiescent oxygen. The theory and operation of the drop generator is discussed by Dabora.[8] The principle of operation is: when a jet of liquid is vibrated at a critical frequency, which depends on the ratio of the jet velocity to the diameter of the jet, the jet breaks up into drops of uniform size and spacing. With proper care all satellite drops may be eliminated. In the earlier phases of the experiments the entire generator chamber was vibrated, while later only the fluid in the generator chamber was vibrated by means of a thin metal diaphragm at the top of the generator.

The combustion of the droplets was initiated by means of a 0.5-in.-i.d. shock tube mounted just below the drop generator at 45° to the combustion tube. For the majority of the tests the driver section of the initiator was filled with 1 atm of stoichiometric hydrogen–oxygen and operated in a detonation mode. This produced a pulse of high-pressure, high-temperature gas traveling behind a Mach 3.5 shock at the exit of the initiator tube. It was found that detonation of the droplets could also be achieved when the driver section of the initiator was pressurized with helium. In that case a Mach 3.9 shock or higher in the 0.5-in.-tube was required for ignition, but, of course, this shock attenuates to a certain extent by the time of contact with the drops.

The instrumentation consisted of space resolved and streak photography, thin film heat transfer gauges, and specially designed pressure transducers. Space resolved schlieren photographs were taken by means of a pulsed, 1-J spark light source synchronized with an electromagnetic shutter[9] to minimize the self-luminous light. Streak photographs were made with an open shutter and a xenon flash tube which was collimated over a portion of the test section. Thin film platinum resistance gauges were used to determine the local heat transfer to the wall. The gauges were coated with a dilute solution of fluorocarbon lacquer for dielectric protection against ionized gases. The output of the gauge, which is proportional to the wall temperature, was integrated numerically by a digital computer and recorded by a digital plotter.

In order to resolve the transient pressures associated with two phase detonations, a piezoelectric transducer with an acoustic absorbing rod[10] was used. In this design, the spurious reflected stress waves within the sensing element are minimized by means of a rod which is attached to the rear surface of the piezoelectric material and which has a matched acoustic impedance. A 0.125-in. diam by 0.050-in. thick disk of lead metaniobate ($PbNb_2O_6$) was used for the sensing element and 0.125-in.-diam by 6-in.-long rod was used as the backup material. The output signal from the pressure transducer was shunted by 0.01 μF and connected directly to an oscilloscope. The response of the pressure transducer flush mounted in the sidewall of a conventional shock tube and in a detonation tube are shown in Fig. 2. The spurious signals are quite small. The slight negative signals in Fig. 2(b) which occur at 120 μsec intervals are identified as the attenuated reflected waves from the end of the tin rod.

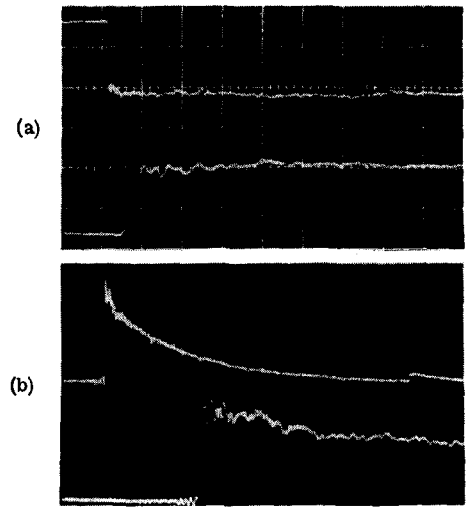

FIG. 2. Response of lead metaniobate transducer. (a) Mach 3.2 normal shock in 1 atm air, 0.02 V/div, 50 μsec/div (upper beam) and 5 μsec/div (lower beam). (b) Stoichiometric hydrogen–oxygen gaseous detonation initially at 1 atm, 0.02 V/div, 100 μsec/div (upper beam) and 10 μsec/div (lower beam).

III. EXPERIMENTAL OBSERVATIONS

Although detonations have been achieved with a variety of drop sizes and mixture ratios, the interest here will be focused upon a single stream of 2600-μ-diam diethylcyclohexane drops which were produced from a 0.063-in. i.d. tube vibrating at 116 Hz. The drops leave the generator with a velocity of about 1.6 ft/sec and spaced 0.17 in. apart thus resulting in a mixture with an equivalence ratio of 2.5. The drops then accelerate to a terminal velocity of 18 ft/sec with a separation distance of 1.85 in. at the optical section and 1.9 in. at 3 ft below the optical section which results in an equivalence ratio of 0.23. Diethylcyclohexane was chosen as the fuel because it is a pure compound of known properties

[8] E. K. Dabora, Rev. Sci. Instr. **38**, 502 (1967).
[9] J. S. Pirroni and R. R. Stevens, Rev. Sci. Instr. **38**, 382 (1967).
[10] K. W. Ragland and R. E. Cullen, Rev. Sci. Instr. **38**, 740 (1967).

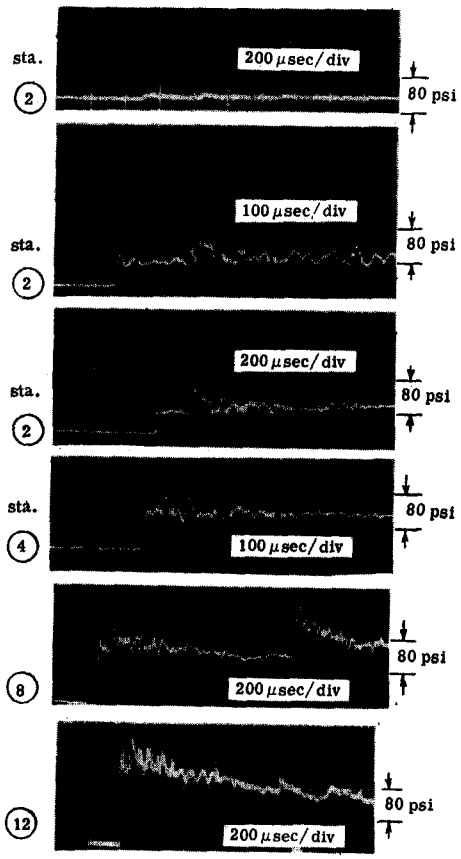

FIG. 3. Pressure records of 2600-μ droplet detonations at selected locations.

with a vapor pressure of less than 2 mm Hg at 20°C. The drops were allowed to fall into a dry tube containing quiescent oxygen for 2–4 sec before the initiator was fired and a photograph of the drops was made 1 sec before each run to insure that the droplet column was properly established.

A. Propagation Velocity and Pressure

Pressure records obtained using the lead metaniobate transducer are shown in Fig. 3 for various positions along the combustion tube. The top trace shows that the pressure pulse due to the driver alone with no drops present is about 10 psi at station 2, and this pulse decays further as it progresses down the tube. With the drops and oxygen gas present detonation is initiated. At station 2 the pressure of the leading shock front jumps to 60 psi and a series of secondary pressure spikes occur about 200 μsec behind the leading shock. These pressure spikes rise at least 100 psi above the local static pressure and are considered to be caused by the local combustion of the wake of the individual drops, which at this station are spaced about 0.6 in. apart. At station 4 the pressure behind the initial shock is 100 psig, and the secondary shocks occur sooner and rise about 50 psi above the local static pressure. The time between secondary shocks is greater because the drops are farther apart. The average velocity between stations 3 and 4 is 2680 ft/sec. At station 8 the initial pressure rise is 150 psi, and the average velocity between stations 7 and 8 is 3120 ft/sec. The second pressure jump at 1200 μsec is discussed after the streak photographs are presented. At station 12 the detonation has traveled 11 ft; the initial pressure rise is 212 psi and the velocity 3850 ft/sec. A reflected shock from the end of the tube appears at station 12 about 1 msec after the leading shock front. Within the experimental error the initial pressure rise agrees with the pressure jump calculated from the normal shock relations using the measured velocity and speed of sound for pure oxygen.

An additional 6-ft extension was added to the tube, and it was found that after the detonation has traveled 16 ft the propagation velocity has reached 4100 ft/sec. This was the maximum length that our space allowed for a vertical tube, but it is felt that a steady-state condition is very nearly reached. It should be noted that for smaller drop sizes at roughly the same equivalence ratio, the steady-state condition is reached sooner.

B. Photographic Description of the Reaction Zone

A spatially resolved schlieren photograph of the detonation front and the zone behind it is shown in Fig. 4. The leading shock front is seen to be quite planar. Behind the front, the drop is seen to be deformed and because the convective flow is supersonic a bow shock as well as wake shocks are visible. The wake (which is deduced to be an origin of combustion from streak photographs shown later) from the upstream drop is swept past the down-

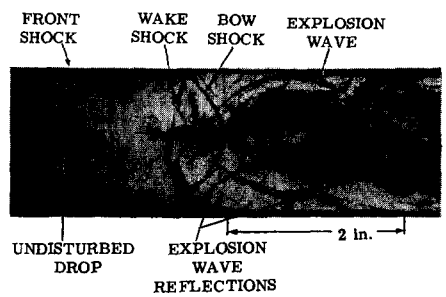

FIG. 4. Schlieren photographs of the reaction zone of 2600-μ droplet detonation.

stream drop and into the as yet unreacted wake. This is the origin of a local explosion and is the source of the strong secondary shock waves observed in the pressure records. The local explosion of the droplet propagates initially in a spherical manner and further stimulates combustion of other droplets. In the lateral direction this local explosion reflects off the walls, while in the logitudinal direction it reinforces the leading shock front. Streak photographs show that the secondary shocks are traveling at 5000 ft/sec just prior to collision with the leading shock front. After a droplet undergoes the local explosion the breakup and burning of the droplet proceed at a more gradual level.

Streak photographs of the detonating column of drops are shown in Fig. 5. In (a) the vertical bright line is an image of the slit with the film stationary. The horizontal band of collimated light yields a shadowgraph effect over a portion of the film. The dark, nearly horizontal line in the collimated light is a drop which happened to be directly in the slit. The leading shock front, traveling at 3350 ft/sec, sweeps over the drops, accelerating and disintegrating them. The light from combustion lags the initial shock by about 65 μsec. The discrete very intense spots of luminosity at the start of the combustion zone are associated with the position of each drop and are caused by intense combustion of the microspray of the wake which is stripped from the parent drop. The combustion of the droplets then proceeds at a more gradual level, and as heat is added to the flow, the angle of the streaks of luminosity gradually decreases indicating a decrease in the convective velocity from 2300 ft/sec initially to 1350 ft/sec after 600 μsec.

Figure 5(b) provides an enlarged view of the drop dynamics. Upon collision with the initial shock, the drop in the collimated light appears to deform instantly, and a bow shock is formed in front of the drop. The separation between the bow shock and the drop increases with time because the drop is deforming laterally. Also the relative velocity between the drop and the convective flow is decreasing slightly due to the acceleration of the drop which also causes the stand off distance of the bow shock to increase. The initial Mach number of the convective flow is 1.40 assuming normal shock conditions, and the Reynolds number based on drop diameter is 2×10^5. The front of the drop is oscillating somewhat behind the bow shock. The dense wake from the drop develops rapidly and grows about 0.8 in. long before it is violently consumed. The intense wake combustion produces a local shock

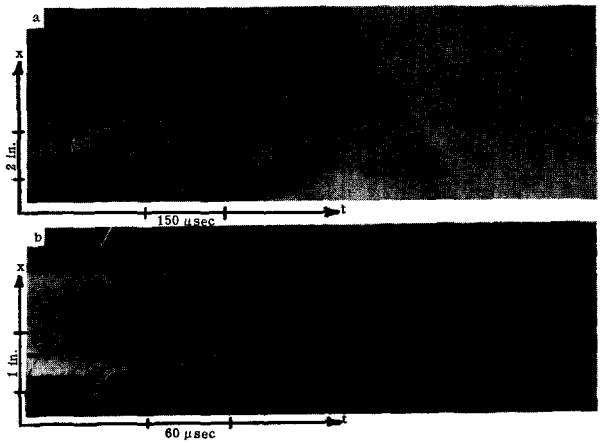

FIG. 5. Self-luminous and shadow streak photographs of 2600-μ droplet detonations.

wave which impinges on the drop just downstream and terminates the bow shock of that drop.

In Fig. 5(a) combustion in the stagnation region at the front of the drop behind the bow shock is just barely visible on the original print. When the detonation wave is observed farther down the tube at a point where the velocity has reached 3750 ft/sec, the stagnation point burning is quite visible (Fig. 6) since the temperature behind the bow shock is higher. According to a one-dimensional, perfect gas estimate the stagnation temperature near the drop before combustion increases from 1550° to 2000°F as the velocity is increased from 3350 to 3750 ft/sec. The stagnation point burning appears distinctly for at least 130 μsec before it is obscured by the rest of the flow.

C. Induced Retonation

In Fig. 5(a) it is apparent that the luminosity continues at the same general level until interrupted by a rearward moving discontinuity; at that point the luminosity increases and at least some of the burning particles change direction and move back up the tube. The velocity of this rearward moving wave as determined by the slope is 3600 ft/sec. This wave is also apparent in the pressure and heat-transfer gauge records. The origin of the disturbance was found to be at the joint between the optical section, which has square corners, and the lower

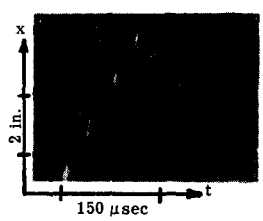

FIG. 6. Streak photograph showing stagnation point burning of 2600-μ drops.

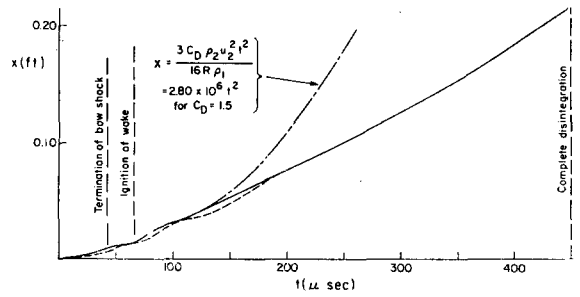

Fig. 7. Displacement of 2600-μ drop versus time after passage of detonation front.

section of the combustion tube, which is structural tubing with rounded corners. In addition to this mismatch there was a slight misalignment. It was found that this rearward moving wave could be eliminated when the joint defect was corrected. An explanation for this effect is that misalignment of the tube produces standing oblique shocks in the convective flow behind the leading shock front of the detonation. As a partially shattered drop flows through the standing shocks, combustion is stimulated with the result that pressure waves are sent out in all directions. The forward moving shocks reinforce the leading detonation shock front while the rearward moving shocks converge and are accelerated by unburned fuel in the reaction zone of the detonation. Thus, we have an induced "retonation" in the analogous sense to what occurs at the transition to detonation in a gas.

As further proof of the ability to induce retonation in this system, a 14-in. long section of tube was added just above the optical section and a plate with a 2.25-in.-diam hole was inserted between the flanges of the original combustion tube and the extra section. The plate triggered a rearward moving shock and caused the propagation velocity to approach its final value sooner. In this way the detonation velocity was increased 400–600 ft/sec in the optical section.

D. Drop Displacement and Disintegration

The displacement of the drop as a function of time after passage of the leading shock front and the complete disintegration time can be obtained from the streak photographs. The drop displacement (from two runs) as a function of time after passage of the shock front is plotted in Fig. 7. During the first 100 μsec of the breakup process the velocity of the leading edge of the drop fluctuates first due to the combustion of the wake of the previous drop and then due to the combustion of the parent wake. A general acceleration of the drop is noted during the first 100 μsec. Between the period of 100–300 μsec the acceleration of the drop is apparently reduced by at least an order of magnitude. It is believed that this is due to an increase in pressure at the rear of the drop as a result of combustion of the wake, and a reduction in the shear stress on the drop because of burning of the upstream surface of the drop. In addition the convective flow is decelerating as heat is added.

Since the density and relative velocity of the convective flow as well as the mass and radius of the drop vary with time after passage of the shock front, the true drag coefficient is difficult to calculate. For the purpose of comparison the displacement of a constant mass drop due to a constant acceleration is also plotted in Fig. 7 assuming that the relative velocity between the drop and the fluid remains at the convective flow behind a normal shock. The area of the drop was based on the initial projected frontal area. A drag coefficient of $C_D = 1.5$ gives good agreement in the early stage of disintegration but large deviation can be observed at a later stage.

The time required for complete disintegration of a 2600-μ droplet due to a two-phase detonation propagating at 3350 ft/sec, as estimated from photographs such as Fig. 5, is 500 μsec. It is interesting to note that at this time the velocity of the drop is only 650 ft/sec, which is 700 ft/sec below the estimated convective velocity and 1840 ft/sec below the initial convective velocity.

A detailed view of the disintegration process of an individual drop during the first 80 μsec after passage of the leading shock front of the detonation is shown in Fig. 8. Each picture is from a different run. Three microseconds after the shock front

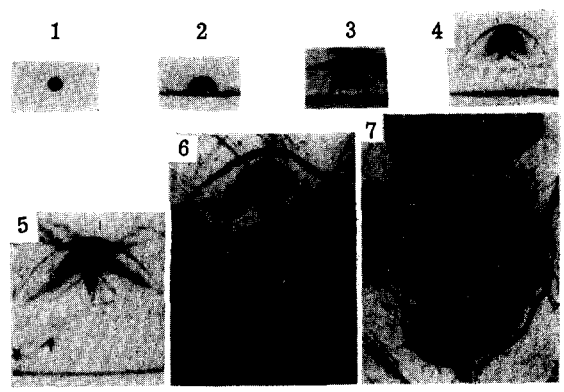

FIG. 8. Schlieren photographs of 2600-μ droplets within the detonation reaction zone 1—undisturbed, 2–3 μsec after contact with the initial shock front, 3–6 μsec, 4–11 μsec, 5–23 μsec, 6–40 μsec, 7–80 μsec.

has made contact with the drop, the drop has flattened appreciably so that the drop appears about 60% wider than the undisturbed drop. In the third and fourth frames of Fig. 8 the establishment of the convective flow about the drop forms a complicated shock structure at the rear of the drop. Some liquid appears to be stripped from the droplet. After 23 μsec the formation of liquid–vapor wake is evident. A wake shock, similar to that observed behind solid spheres, is also clearly seen; in this case the rapid vaporization of the microspray in the wake may accentuate the wake shock. The final frame of Fig. 8 shows the explosion of the wake.

A number of investigators have studied the dynamic behavior of single, inert droplets in shock tubes.[11–13] The tendency of the dynamic pressure ($\frac{1}{2}\rho u^2$) of the convective flow behind a shock wave to distort the drop is opposed by inertia, surface tension, and viscous stress within the drop. For high-speed flow such as encountered in two phase detonations, it is believed that surface tension and viscous forces may be neglected compared to the inertia. Just as in the burning case (Fig. 8), the inert drop flattens out to several times the initial diameter and material is stripped from the outer edge of the drops.[14]

As shown by Clark[15] for the breakup of liquid jets, the breakup time t_b may be correlated to the experimental data by the expression

$$t_b = \frac{\epsilon\, d}{u(\rho_g/\rho_l)^{\frac{1}{2}}},$$

where d is the initial diameter of the drop, u is the convective velocity, ρ_g is the density of the gas, ρ_l is the density of the liquid, and ϵ represents the relative distortion of the drop. For liquid jets[15] and drops with dynamic pressures q below 2 atm, ϵ may be taken as constant and equal to 12. However, there is some evidence that ϵ is lower for inert drops when the dynamic pressure is 20 atm.[11] For the 2600-μ droplet detonation experiments $\epsilon = 14$ and $q = 21$ atm based on the initial conditions behind the shock. Of course, if average conditions within the two-phase detonation were used, q would be lower.

[11] A. A. Ranger and J. A. Nicholls, A.I.A.A. J. (to be published).

[12] W. H. Andersen and H. E. Wolf, in *Proceedings 5th International Shock Tube Symposium* (U. S. Naval Ordinance Laboratory, Silver Spring, Maryland, 1965), p. 1145.

[13] O. G. Engle, J. Res. Natl. Bur. Std. (U. S.) **60**, 245 (1958).

[14] When the dynamic pressure is very low such that it is of the order of the surface tension pressure a different type of breakup is observed, which is termed "bag type" (i.e., the drop inflates like a parachute until it bursts in the center). At still lower dynamic pressures the drop vibrates with increasing amplitude until it breaks up.

[15] B. J. Clark, NASA Technical Note D-2424 (1964).

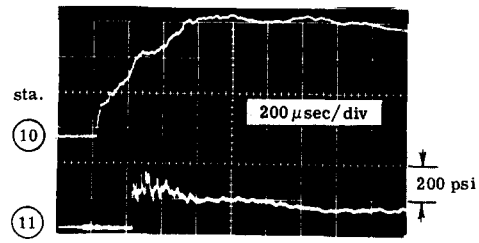

FIG. 9. Response of thin-film heat-transfer gauge (upper) and pressure transducer (lower) to 2600-μ droplet detonation.

E. Heat Transfer to the Walls

Thin-film heat-transfer gauges were used to estimate the extent of the reaction zone and to determine the percent of the heat release which is lost from the reaction zone. A representative wall temperature record is shown in Fig. 9 where a pressure trace is also included. In general, at stations 10 and 12 the wall temperature increase during the first 600–800 μsec and then levels out at 300 to 400°F. A constant wall temperature implies that the heat transfer to the wall is decreasing as $t^{-\frac{1}{2}}$. The heat transfer rate, which was obtained by integrating the wall temperature data, is shown in Fig. 10 for four different runs. At stations 10 and 12 the heat transfer to the wall shows large fluctuations for the first 600–800 μsec after passage of the initial shock front which is not unreasonable in view of the discrete combustion zones, turbulence, and secondary shocks. The average heat transfer rate is near 1000 Btu/ft^2-sec during the first 600–800 μsec and then decreases markedly and the fluctuations diminish. At about 1500 μsec the reflected shock from the end

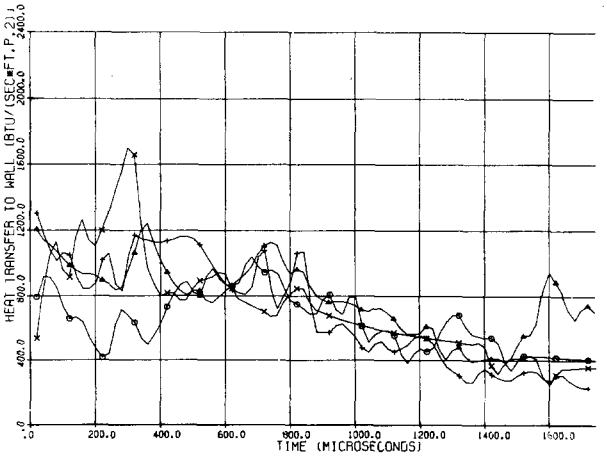

FIG. 10. Heat transfer to the wall at station 12 for the 2600-μ-diam droplet denotations.

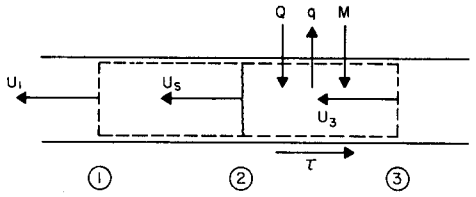

FIG. 11. Control volume for the one-dimensional analysis.

of the combustion tube terminates the useful data. At station 8 the heat transfer is considerably lower since the detonation is less fully developed and a value of 350 Btu/ft^2-sec is maintained for 1200 μsec, at which point the "retonation" appears.

On the basis of the wall temperature and heat transfer data, it is felt that on the average the chemical heat release is completed after 670 μsec or about 2.5 ft behind the initial shock front. That is to say, the point where the wall temperature becomes nearly constant, which occurs at 600–800 μsec depending on the particular run, is taken as the point where chemical reaction is completed. After 600–800 μsec the heat transfer decreases more rapidly than the $t^{-1/7}$ or $t^{-1/5}$ variation which would be expected for a turbulent boundary layer with constant free-stream properties. This interpretation is also borne out by the pressure records. After the initial jump the pressure oscillates and increases slightly for about 200 μsec due to the generation of secondary shocks and then decreases due to heat addition.

Assuming that 1000 Btu/ft^2-sec is lost out of the reaction zone for 670 μsec and assuming a heat of reaction of 16 200 Btu/lb-fuel, the experiments on the 2600-μ-diam drops indicate that approximately 20% of the heat release is lost to the walls. The influence of losses from the reaction zone on the steady-state properties of a two-phase detonation are considered in the next section.

IV. ONE-DIMENSIONAL THEORY

The propagation velocity u_s, the equilibrium pressure p, density ρ, temperature T, and speed of sound a, at the end of the reaction zone of a two-phase detonation may usefully be approximated by the Rankine–Hugoniot relations with the Chapman–Jouguet condition in a manner analogous to that used for gaseous detonations provided that the liquid phase is properly taken into account. For a dilute spray one may keep the gas phase and the liquid phase separate and define the equation of state and speed of sound in terms of the gas phase,[16] or one may use a one-fluid model with effective thermodynamic properties of the mixture.[5] However, because of the extended reaction length in two-phase detonations, it is desirable to also include the effect of drag and heat loss from the reaction zone, as will be shown below.

The presentation is restricted to one-dimensional theory so that the mass, momentum, and heat transfer which occur at the boundaries are assumed to be uniformly distributed over the entire cross-section area of the tube. This point of view was originally proposed by Zeldovich[17,18] in an attempt to account for the reduction in the velocity of propagation of gaseous detonations as the tube diameter is decreased. However, sufficient data were not available at that time to quantitatively evaluate the method. Fay[19] proposed that the correct physical picture was that the divergence of the streamlines due to the displacement thickness of the boundary layer (which is negative behind a shock or detonation) caused the velocity deficit. Fay's calculations gave reasonably good agreement with measured results for various gaseous detonations in tubes with a 1-cm radius. In essence the two methods are similar except that Fay's approach does not explicitly account for the heat loss to the walls. The first approach is used because the heat transfer (and assuming Reynolds analogy holds, also the drag) can readily be measured for the two-phase detonations while the displacement thickness cannot. In the Appendix this approach is shown to yield satisfactory results for the velocity deficit observed with gaseous detonations.

Consider a column of gas in a tube between an initial condition, $x = x_1$ and an equilibrium condition $x = x_3$ which contains a shock discontinuity at $x = x_2$. Heat and mass addition, shear stress, and heat loss at the boundaries occur between x_2 and x_3 as shown in Fig. 11. For a time steady flow either wall fixed (i.e., laboratory) or shock-fixed coordinates may be used. The transformation from the laboratory coordinate x to the shock-fixed coordinate $\bar{x}$ is given by $\bar{x} = u_s t - x$, where u_s is the shock velocity and t is the time. The velocity transformation between the shock-fixed and the laboratory coordinates is $\bar{u}_i = u_s - u_i$, where i can be 1, 2, or 3 and u_i refers to velocity with respect to laboratory coordinates. Choose a control volume which contains the gas between x_1 and x_3. The drops

[16] F. A. Williams, in *Progress in Astronautics and Rocketry* (Academic Press Inc., New York, 1962), Vol. 6, p. 99.

[17] Ia. B. Zeldovich, Zh. Eksp. Teor. Fiz. 10, (1940) [NACA TM 1261 (1950)].

[18] Ia. B. Zeldovich and A. S. Kompaneets, *Theory of Detonation* (Academic Press Inc., New York, 1960), p. 133.

[19] J. A. Fay, Phys. Fluids 2, 283 (1959).

remain outside the control volume. It is assumed that all of the liquid is consumed and enters the control volume before the end of the reaction zone at station 3.

The conservation of mass, momentum, and energy are

$$\rho_3\bar{u}_3 - \rho_1\bar{u}_1 = \phi\rho_1\bar{u}_1, \tag{1}$$

$$\rho_3\bar{u}_3^2 - \rho_1\bar{u}_1^2 - \phi\rho_1\bar{u}^2 = p_1 - p_3 - \frac{b}{A_c}\int_{x_2}^{x_3} \tau\, dx, \tag{2}$$

$$\rho_3\bar{u}_3\left(e_3 + \frac{\bar{u}_3^2}{2}\right) - \rho_1\bar{u}_1\left(e_1 + \frac{\bar{u}_1^2}{2}\right) - \left(e_l + \frac{\bar{u}_1^2}{2}\right)\phi\rho_1\bar{u}_1$$

$$= p_1\bar{u}_1 - p_3\bar{u}_3 + \phi\,\Delta H\rho_1\bar{u}_1 - \frac{b}{A_c}\int_{x_2}^{x_3}(q - \tau u_s)\, dx, \tag{3}$$

where ϕ is the fuel to oxygen mass oxygen mass ratio, A_c is the cross-sectional area of the tube, τ is the shear stress at the wall, e is the internal energy, ΔH is the heat of reaction per unit mass of fuel, q is the heat loss to the surface of the tube per unit area per second, and b is the perimeter of the tube. The ϕ terms in Eqs. (1) and (2) and the first ϕ term in Eq. (3) are due, of course, to the presence of the liquid phase. It should be noted that the drag force of the drops on the gas is not included because momentum which is lost to the drops is added by the incoming vapor from the drops, and similarly the heat lost to the drops is returned to the system in the form of increased internal energy of the vapor.

Let us now assume that (a) the fluid is initially at rest, i.e., $u_1 = 0$. (b) The Chapman–Jouguet condition holds at position $\bar{x}_3$, i.e., $\bar{u}_3 = a_3$. (c) The gases are both thermally and calorically perfect so that,

$$h = C_pT = \frac{a^2}{\gamma - 1} \quad \text{and} \quad a^2 = \frac{\gamma p}{\rho} = \gamma RT.$$

Let us also for convenience, introduce mean transfer coefficients based on the flow conditions in laboratory coordinates

$$C_D \equiv b\int_{x_2}^{x_3} \tau\, d\bar{x}(\tfrac{1}{2}A_s\rho_2u_2^2)^{-1}, \tag{4}$$

$$C_H \equiv b\int_{x_2}^{x_3} q\, d\bar{x}\left[A_s\rho_2u_2\left(h_2 + \frac{u_2^2}{2} - h_w\right)\right]^{-1}. \tag{5}$$

In terms of ρ, a, and u_s the extended Rankine–Hugoniot equations for a two-phase Chapman–Jouguet detonation become

$$\rho_3a_3 - \rho_1u_s = \phi\rho_1u_s, \tag{6}$$

$$\rho_3a_3^2\left(\frac{\gamma_3 + 1}{\gamma_3}\right) - \rho_1\left(u_s^2 + \frac{a_1^2}{\gamma_1}\right) = \left(\phi + \frac{C_DA_su_2}{2A_cu_s\bar{u}_2}\right)\rho_1u_s^2, \tag{7}$$

$$\rho_3a_3^3\left(\frac{\gamma_3 + 1}{\gamma_3 - 1}\right) - \rho_1u_s\left(\frac{2a_1^2}{\gamma_1 - 1} + u_s^2\right)$$

$$= \left[(u_s^2 + 2e_M)\phi + C_D\frac{A_su_2^2u_s^2}{A_cu_s\bar{u}_s} + \phi\,\Delta H - C_H(h_1 + u_su_2 - h_w)\frac{A_su_2}{A_c\bar{u}_2}\right]\rho_1u_s. \tag{8}$$

From Eqs. (6) and (7) and the relation $p = \rho a^2/\gamma$, expressions for the pressure, speed of sound, density, and temperature ratios across the detonation can be written in terms of the Mach number of propagation as follows:

$$\frac{p_3}{p_1} = \frac{\gamma_1M_s^2(1 + \phi)}{1 + \gamma_3}Z, \tag{9}$$

$$\frac{a_3}{a_1} = \frac{\gamma_3M_s}{1 + \gamma_3}Z, \tag{10}$$

$$\frac{\rho_3}{\rho_1} = \frac{(1 + \gamma_3)(1 + \phi)}{\gamma_3}\frac{1}{Z}, \tag{11}$$

$$\frac{T_3}{T_1} = \frac{\gamma_3\gamma_1m_3M_s^2}{(1 + \gamma_3)^2m_1}Z^2, \tag{12}$$

where

$$Z = 1 + \frac{1}{\gamma_1M_s^2(1 + \phi)} + \frac{C_DA_su_s^2}{2(1 + \phi)A_cu_s\bar{u}_2}.$$

In order to obtain an expression for the Mach number of propagation in terms of the transfer coefficients, heat release, etc., one must also include Eq. (8) which after considerable manipulation yields a fourth-order algebraic equation

$$M_s^4\left[(1 + \phi)^2 + \frac{C_DA_su_2^2(1 + \phi)}{A_cu_s\bar{u}_2} + \left(\frac{\gamma_3C_DA_su_2^2}{2A_cu_s\bar{u}_2}\right)\right]$$

$$+ 2M_s^2\left[\left(\frac{\gamma_3^2}{\gamma_1} - \frac{\gamma_3^2 - 1}{\gamma_1 - 1}\right)(1 + \phi)\right.$$

$$- \frac{(\gamma_3^2 - 1)(\phi + \phi^2)(\Delta H + e_M)}{a_1^2}$$

$$+ \frac{(\gamma_3^2 - 1)(1 + \phi)C_H(h_1 + u_su_2 - h_w)A_su_2}{a_1^2A_c\bar{u}_2}$$

$$\left. + \frac{\gamma_3^2C_DA_su_2^2}{2\gamma_1A_cu_s\bar{u}_2}\right] + \frac{\gamma_3^2}{\gamma_1^2} = 0. \tag{13}$$

Of course, $u_2^2/u_s\bar{u}_2$ is a function of M_s, but it varies quite slowly. For a perfect gas with $\gamma_1 = 1.4$, the normal shock relations can be shown to yield,

$$\frac{u_2^2}{u_s\bar{u}_2} = \frac{25(M_s^2 - 1)^2}{6M_s^2(M_s^2 + 5)}. \tag{14}$$

By considering the order of magnitude of the terms in Eq. (13) and by letting $h_1 - h_w = 0$, a useful approximation, which for experimental conditions is only about 4% high, is

$$u_s^2 = a_1^2 M_s^2 = \frac{2(\gamma_3^2 - 1)\phi\ \Delta H}{1 + \phi + (C_D A_s u_2^2/A_c u_s \bar{u}_2) + [2(\gamma_3^2 - 1)C_H A_s u_2^2/A_c \bar{u}_2 u_s]}. \tag{15}$$

The heat of reaction ΔH should be obtained from a solution of Eqs. (1)–(3) with the thermodynamic variables obtained from a reacting mixture of gases in equilibrium. Computer solutions of this type[20] are available for the case where $C_D = C_H = 0$. As a first-order solution for the reduction in the propagation velocity due to drag and heat loss at the boundaries of the reaction zone, we may denote $(u_s)_0$ as the detonation velocity without losses, where

$$(u_s)_0^2 = 2(\gamma_3^2 - 1)\phi\ \Delta H/(1 + \phi) \tag{16}$$

and then Eq. (15) becomes

$$\frac{u_s}{(u_s)_0} = \left\{1 + [C_D + 2(\gamma_3^2 - 1)C_H] \cdot \left(\frac{1}{1+\phi}\right)\left(\frac{A_s}{A_c}\right)\left(\frac{u_2^2}{u_s \bar{u}_2}\right)\right\}^{-\frac{1}{2}}. \tag{17}$$

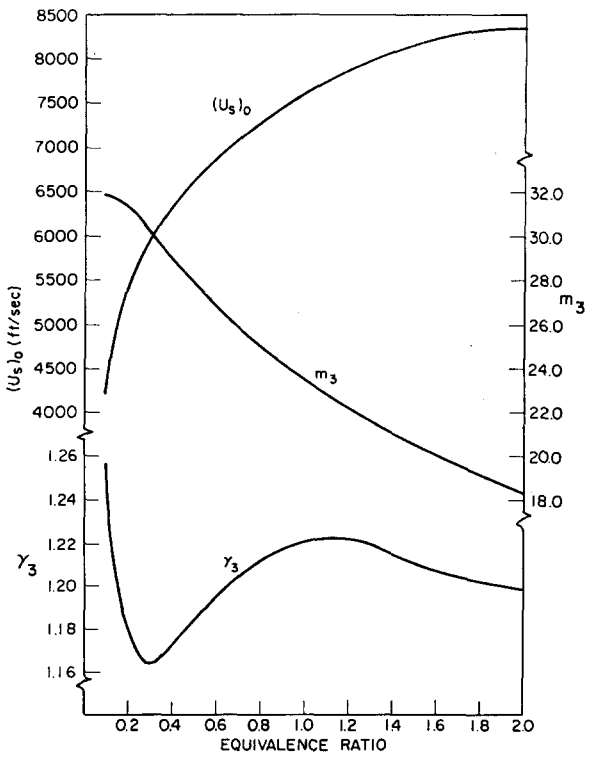

FIG. 12. Theoretical propagation velocity, molecular weight, and ratio of specific heats for a gaseous diethylcyclohexane—oxygen detonation.

[20] F. J. Zeleznik and S. Gordon, NASA Technical Note D 1454 (1962).

The calculated values of $(u_s)_0$, γ_3, and the molecular weight m_3, for a Chapman–Jouguet detonation of gaseous diethylcyclohexane and oxygen initially at 1 atm and 20°C are plotted in Fig. 12.

Comparison of Theory and Experiment

Equations (9) and (17) for the Chapman–Juoguet pressure ratio and the velocity deficit may be compared directly with the experimental results. For the experiments $A_s/A_c = 16u_s t_3/b$, and the perimeter b was 0.536 ft. For the 2600-μ drops the average value of t_3 was 670 μsec (based on the time required for the platinum resistance gauge to level off). The average total heat-transfer coefficient [defined by Eq. (5)] was 1.8×10^{-3}. The drag coefficient for the walls of the tube was obtained by assuming that the Reynolds analogy holds so that $C_D = 2C_H$.

Before proceeding with the comparison of theory and experiment it is worth comparing the value of C_D obtained by use of the Reynolds analogy with other data. The transition Reynolds number in conventional shock tubes[21] is about 0.8×10^6. Since combustion is known to greatly reduce transition and since the inherent structure of detonation is conducive to turbulence, one can assert that the boundary layer in the reaction zone is turbulent. The Reynolds number based on the length of the reaction zone and conditions immediately behind the shock front is 3×10^8 where Re is defined[22] as

$$\mathrm{Re} = u_2^2 x/\nu \bar{u}_1.$$

If conditions at the end of the reaction zone are used to evaluate the Reynolds number, then approximately half the above value would be obtained, so that there is no doubt that the Reynolds number exceeds the transition Reynolds by two orders of magnitude. Furthermore, Martin[22] found that for $\mathrm{Re} = 8 \times 10^7$, $M_s = 2.65$, and $p_1 = 120$ mm Hg, the local skin friction coefficient was 1.6×10^{-3} and a $\frac{1}{7}$ power profile gave good correlation of the data. If his data are extrapolated to our conditions, we obtain $C_D = 1.5 \times 10^{-3}$. Similar results would

[21] J. C. Breeze and C. C. Ferriso, Phys. Fluids 7, 1071 (1964).

[22] I. I. Glass and G. J. Hall, in *Handbook of Supersonic Aerodynamics: Shock Tubes* (U. S. Government Printing Office, Washington, D. C., 1959), Vol. 6, Sec. 18.

be obtained from Schlichting's[23] equation $C_D = 0.074\ \mathrm{Re}^{-1/5}$. It is concluded that because of the combustion and the secondary shocks in our experiments the value of $C_H = C_D/2 = 1.8 \times 10^{-3}$ is not unreasonable.

The measured and calculated pressure ratio, velocity deficit, and estimated Chapman–Jouguet velocity are compared in Table I. The pressure ratio at 670 μsec after passage of the shock front, which is the estimated end of the reaction zone, is shown for several representative runs. The pressure ratio has decreased from a normal shock pressure ratio of 15.4–12.1 after heat addition, for example. The next three rows show, respectively, the equivalent all gaseous case, the effect of mass addition, and the effect of mass addition plus frictional and heat losses at the boundaries. Since the mixture ratio is relatively lean, mass addition results in only a small increase in the pressure ratio at the end of the reaction zone for a fixed velocity of propagation. Accounting for the effect of drag increases the pressure ratio further and yields fairly good agreement with the measured results.

The measured propagation velocity for a representative condition is 32% below the equivalent gaseous case. Theoretically, mass addition does not change u_s. However, when drag and heat loss at the boundaries are considered, nearly all the velocity degradation is taken into account.

The convective velocity at t_3 was estimated from the streak photographs and compared to Eq. (10) with $a_3 = u_s - u_3$. Although the convective velocity is at best difficult to obtain from the photographs, it is worth noting that theoretically the effect of mass addition is to slightly raise u_s, but drag on the walls reduces u_3 rather drastically. Since two-phase detonations are extended several orders of magnitude compared with gaseous detonations, further attempt to examine the Chapman–Juoguet condition might prove fruitful.

TABLE I. Comparison of theory and experiment for representative runs.

u_s (ft/sec)[a]		3300	3710	3900	3700	3750
p_2/p_1 meas.		11.0	12.0	12.6	12.1	
calc. [Eq. (9)]	(a)	6.8	8.3	9.2	9.0	
	(b)	7.2	8.9	9.8	9.6	
	(c)	9.1	11.7	13.1	12.9	
$u_s/(u_s)_0$ meas.				0.68		
calc. [(Eq. (17)]	(a)			1		
	(b)			1		
	(c)			0.71		
u_3/a_1 meas.						1.3
calc. [(Eq. (10)]	(a)					1.5
	(b)					1.5
	(c)					1.0

[a] (a) $\phi = C_D = C_H = 0$,
(b) $\phi = 0.067$, $C_H = C_D = 0$,
(c) $\phi = 0.067$, $C_H = C_D/2 = 1.8 \times 10^{-3}$.

V. SUMMARY

It has been demonstrated that a detonation wave can propagate in a tube containing a single stream of 2600-μ-diam fuel droplets dispersed in gaseous oxygen. While the end result in this type of detonation is analogous to that of a gaseous detonation, the reaction zone thickness is several orders of magnitude larger than that of a gaseous detonation due to deformation, stripping, vaporization, and diffusion of the liquid fuel. Under the experimental conditions the detonation wave reached a nearly steady velocity of 4100 ft/sec after 16 ft. The leading shock front was quite planar and gave a steep fronted pressure rise which agreed with normal shock relations for pure oxygen. Secondary shocks were observed followed by a gradual decrease in pressure as the heat release occurred.

Photographs of an individual drop within the reaction zone show that deformation and stagnation point burning of the droplet start almost immediately after contact with the leading shock front. A bow shock is formed about the drop, and the drop disintegrates gradually over a period of 500 μsec while undergoing a displacement of 0.20 ft. At first the stripped microspray in the wake of the drop reacts very little, but when the hot combustion products of the neighboring upstream droplet flow through the wake of the unreacted fuel mist, a localized explosion of the wake occurs. Strong secondary explosions were also observed near the initiator where the propagation velocity was lower, and thus provide a powerful means of accelerating the detonation front. Combustion of the wake of the disintegrating droplet then proceeds more gradually for a period of the order of 670 μsec. During this time approximately 20% of the heat of reaction is lost to the walls of the tube.

One-dimensional equations for a Chapman–Jouguet detonation wave with mass and heat addition within the reaction zone, and momentum and heat transfer out of the reaction zone were derived and applied to the experimental conditions. The theory is shown to be a useful approximation for the propagation velocity and the conditions at the end of the reaction zone of the two-phase detonation.

[23] H. Schlichting, *Boundary Layer Theory* (McGraw-Hill Book Company, New York, 1960), p. 537.

TABLE II. Comparison of calculated and measured velocity deficits for gaseous detonations.

Composition	Velocity (m/sec)	Re (10^6)	C_D (10^{-3})	X (cm)	γ_3	$\Delta u/(u_s)_0$ (meas)	$\Delta u/(u_s)_0$ (calc)	$\Delta u/(u_s)_0$ (Fay's calc)
$2H_2 + O_2$	2830	0.67	4.8	0.35	1.29	1.2%	1.0%	1.0%
$2H_2 + O_2 + 5He$	3660	1.8	3.9	0.98	1.56	2.5	2.9	2.2
$2H_2 + O_2 + 13He$	3823	2.4	3.7	1.80	1.62	4.4	4.9	3.3
$2H_2 + O_2 + 13A$	1522	3.0	3.6	0.86	1.62	2.7	2.5	1.6
16% H_2 + 84% Air	1552	2.8	3.6	0.73	1.36	1.6	1.1	1.4

ACKNOWLEDGMENTS

The authors are indebted to R. E. Cullen for his participation in the early phases of this study. D. F. Giere, R. C. Stitt, and H. D. Radcliff ably assisted with the experiments.

This work was supported by the National Aeronautics and Space Administration Lewis Research Center under Contract NASr 54(07).

APPENDIX

Fay[19] has calculated the detonation velocity deficit for various mixtures in a 1-cm-radius tube initially at 1 atm according to the scheme that he developed using the boundary-layer displacement thickness. For this purpose Fay used Gooderum's[24] interferometric measurements of the turbulent boundary in a shock tube. He compared his calculations to certain experimental measurements that were extrapolated or interpolated to the same conditions. It is of interest to calculate the velocity deficit for these gaseous detonations by means of Eq. (17) using the same conditions and values, where possible, as were used by Fay.

For gaseous detonations in a circular tube, and assuming that $C_H = \frac{1}{2}C_D$, Eq. (17) reduces to

$$\frac{\Delta u}{(u_s)_0} = 1 - \left[1 + 2C_D\gamma_3^2 \frac{u_2^2}{u_s\bar{u}_2}\frac{X}{R}\right]^{-\frac{1}{2}}, \qquad (18)$$

where Δu is the velocity deficit, X is the reaction zone thickness, and R is the tube radius. When $\Delta u/(u_s)_0 \ll 1$ Eq. (18) reduces to

$$\frac{\Delta u}{(u_s)_0} = C_D\gamma_3^2 \frac{u_2^2}{u_s\bar{u}_2}\frac{X}{R}. \qquad (19)$$

Thus the velocity deficit is proportional to X/R and, since C_D varies approximately as $\mathrm{Re}^{-1/7}$, we have the same functional form as in Fay's analysis.

The total drag coefficient, C_D within the reaction zone of gaseous detonations has not been measured. Therefore Martin's[22] interferometric measurements for a turbulent boundary layer behind a plane shock wave were used to estimate C_D. Since Martin's experiments were for Reynolds numbers from 10^7–10^8, his data were extrapolated according to a $\frac{1}{7}$ power law, and the Reynolds number was based on conditions immediately behind a normal shock traveling at the detonation velocity. If estimated average conditions within the reaction zone had been used the Re would be lower and therefore C_D higher. Values used for the viscosity and reaction zone thickness are taken from Fay's paper.

The calculated and measured velocity deficits and the assumed quantities for stoichiometric hydrogen–oxygen, stoichiometric hydrogen–oxygen diluted with helium and argon, and hydrogen–air are summarized in Table II. The calculated velocity deficit using Eq. (19) correctly predicts the trend of the experimental data and considering the uncertainties yields excellent agreement. It is concluded that either the method which accounts for the drag and heat loss at the boundaries, or the method which utilizes the displacement thickness of the boundary layer may be used to calculate the detonation velocity deficit of a detonation wave.

[24] P. B. Gooderum, NACA Technical Note 4243 (1958).